ISSN 2250-3153

# Effect of Force Control during Spot Welding on Weld Properties

**Aravinthan Arumugam[*] and Abdul A Baharuddin[**]**

[*]School of Engineering, KDU University College, Jalan SS22/41, Damansara Jaya, 47400 Selangor, MALAYSIA
[**]Department of Mechanical, Materials and Manufacturing Engineering, University of Nottingham Malaysia Campus, Jalan Broga, Semenyih, 43500 Selangor, MALAYSIA

***Abstract-*** Resistance Spot Welding (RSW) is a process that is widely used in the automotive industries. The parameters that are used to develop a spot weld are the welding current, weld time and electrode force. Electrode force was not used as a control parameter due to the use of pneumatic system to actuate the welding electrode. The pneumatic system does not allow the development of closed loop control system; therefore electrode force was not used to control the growth of the spot weld nugget. This reported work looks into the ability to control electrode force dynamically during welding by using servomechanism. Force profiles were introduced in this work and the electrode force during welding was controlled to follow these force profiles. Based on the findings, the developed controller was able to control the electrode force during welding to follow the given force profiles. Decreasing the electrode force during welding facilitates the initiation of spot weld growth earlier in the weld cycle which in turn produces bigger weld diameter and stronger weld strength. The opposite was noticed when electrode force was increased during the weld cycle. Furthermore decreasing the electrode fore during welding produced a button pull-out failure and increasing the force produced an interfacial weld failure.

***Index Terms***- Electrode force, Dynamic resistance, Weld diameter, Weld strength, Failure mode

## I. INTRODUCTION

Resistance spot welding (RSW) is a process used to join sheet metal parts by means of a series of spot welds. This process is extensively used in mass production of automotive, metal furniture and appliances. Automotive manufacturing uses about 4000 – 6000 spot welds for an automotive body which is known as body-in-white (BIW). As a large number of spot welds are required for an automotive body to bear the various types of loadings that the automotive will be subjected to, the manufacturing cost for the spot welding process has increased tremendously. In addition, issues related to quality of spot welds are still being faced by the industries. Spot weld quality can be categorized in terms of the weld strength and weld nugget diameter. Stringent quality control will not only improve the quality of each spot weld but will also reduce the amount of spot welds required for an automotive hence reducing the cost significantly. The three main parameters that govern spot weld quality are current, time and force. Proper control of these parameters will generate the required heat for melting the metal and development of spot weld nugget. Increase in spot weld nugget diameter has been shown to increase spot weld strength [1]. Increase in the welding current was found to increase the weld nugget diameter, which in turn increases the weld strength until expulsion occurs [2]. Similarly increase in weld time also increases weld nugget diameter and weld strength until occurrence of expulsion [3]. Expulsion is a phenomenon that occurs when molten metal is expelled from the weld zone during welding, due to force caused by weld nugget expansion (growth) exceeds the supplied electrode force. On the other hand, decrease in electrode force will increase the weld nugget diameter and the weld strength until expulsion occurs [4]. For decades current and time have been the vital control parameters in the industry due to the availability of electronic controllers which allow the development of closed loop control system. Electrode force was not a control parameter because of the use of the pneumatic system to supply force during welding. Pneumatic system, being a mechanical system, does not allow the development of a closed loop control system; therefore force could not be monitored or controlled during spot welding [5]. The objective of this work is to control the electrode force using a servo-based system and to study the effect of controlling electrode force at a predetermined pattern to the weld growth, weld strength and weld failure mechanism.

*Importance of Electrode Force*

Electrode force plays a huge role in the heat generation during the spot welding process according to equation,

$$Q = I^2 \times R \times t;$$

where Q = heat generated (kJ), I = welding current (kA), R = resistance (Ω) and t = weld time (cycles – 1 cycles = 20 ms for a 50 Hz spot welding machine). The electrode force affects the heat generation by controlling the resistance during the welding process. During the squeeze cycle, the electrode force which is used to bring the metal sheets into contact influences the contact resistance between the sheets or also known as faying surfaces. The contact resistance stems from the presence of roughness on the contact surfaces or an additional layer between contact surfaces. Contact resistance can be increased by reducing electrode force which will reduce the contact area at the faying surfaces and increase the current density [6]. This will produce higher heat generation and increases the rate of melting of material during spot welding for a given welding current and weld time [7]. During the weld cycle, electrode force influences the dynamic resistance, which produces the Joule heating required for spot weld growth. The dynamic resistance during

RSW is a result of the sum of the bulk resistance, constriction resistance and film resistance and dominance of each resistance may change during the welding sequence [8]. The dynamic resistance during welding was reported to correlate well to the weld nugget growth as shown in Figure 1 [9]. The β-peak indicates the start of weld nugget growth. Dynamic resistance was found to decrease with an increase in electrode force during welding [10]. The delay in formation of the β-peak at higher electrode force also indicates a delay in the initiation of weld nugget growth due to the reduction in Joule heating. This shows that the ability to control the electrode force during the weld cycle would be able to control the spot weld growth and also further improves the strength of the spot weld.

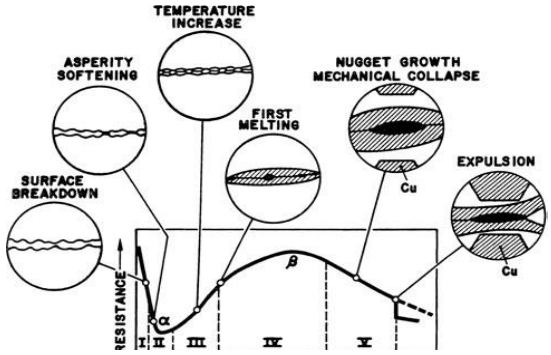


**Figure 1: Dynamic resistance during spot welding [9]**

*A. Instrumentation*

A pedestal type welding machine (WIM-75 kVA) with pneumatic based electrode actuation system was retrofitted in this work, into a servo-based electrode actuation system. Instead of the pneumatic piston, which was used to bring the electrode upwards and downwards, a ball screw was used to convert the rotary motion of the servomotor to a linear motion so that the electrode can be actuated upwards and downwards. A piezoelectric force-strain sensor was fitted to the lower arm of the machine to measure the applied electrode force based on the strain at the lower arm. This is due to the infeasibility of measuring the electrode force directly from the electrode tip during the welding process. This sensor was used to produce a feedback signal of the electrode force in order to develop a closed loop control system. The electrodes used in this work are RWMA Class II CuCr alloy electrodes with tips of 6 mm in diameter. Test samples for metallographic study and tensile tests were prepared from mild steel plates (BS1449) with dimensions of 100 mm x 30 mm and thickness of 2 mm.

*B. Force Control System*

A proportional-integral-derivative (PID) controller was developed to control the electrode force during weld cycle based on force profiles. The force profiles are function of time, P(t). Each force profile consists of a series of force values for each half cycle (10 ms), $P(t_i)$ throughout the entire weld time. Details on the force profiles will be discussed in the subsequent section. Feedback signal from the force-strain sensor for every half cycle, $P(t_i)$' will be compared with the respective $P(t_i)$ value from the force profile to generate an error signal, $e(t_i)$. The error signal will be sent to the PID controller which in turn, sends a low energy signal in the range of ±10 V to the motor amplifier. The motor amplifier will then produce the required current to drive the servo motor. The torque of the servo motor will be converted to a force by the mechanical components (ball screw and gearbox) and sent to the electrode to change the electrode force accordingly, as shown in Figure 2.

*C. Force Profiles*

The welding current and weld time were selected as 10 kA and 40 cycles (800 ms) respectively. Figure 3 shows the force profiles that were used in this work. The force profiles were chosen based on certain characteristics and it was intended to evaluate how these different force profiles affect the spot weld properties. The weld properties in this work refer to weld diameter, weld strength and mode of failure of weld. Force profile A is a force profile which has a higher electrode force (2.5 kN) at the start of the weld cycle but decreases to a lower electrode force (1.5 kN) during the weld cycle and maintains the force till the end of the weld cycle. Force profile B refers to a constant electrode force of 2.5 kN throughout the whole weld cycle. Force profile C refers to a force profile which has a lower electrode force (2.5 kN) at the start of the weld cycle but increases to a higher electrode force (3.5 kN) during the weld cycle and maintains the force till the end of the weld cycle. In force profiles A and C, at 100 ms, force starts to ramp down and ramp up respectively at a rate of 1 kN/100ms.

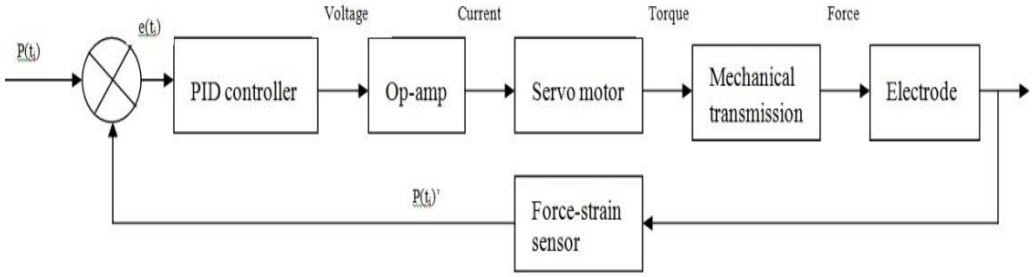


**Figure 2: Force control diagram**

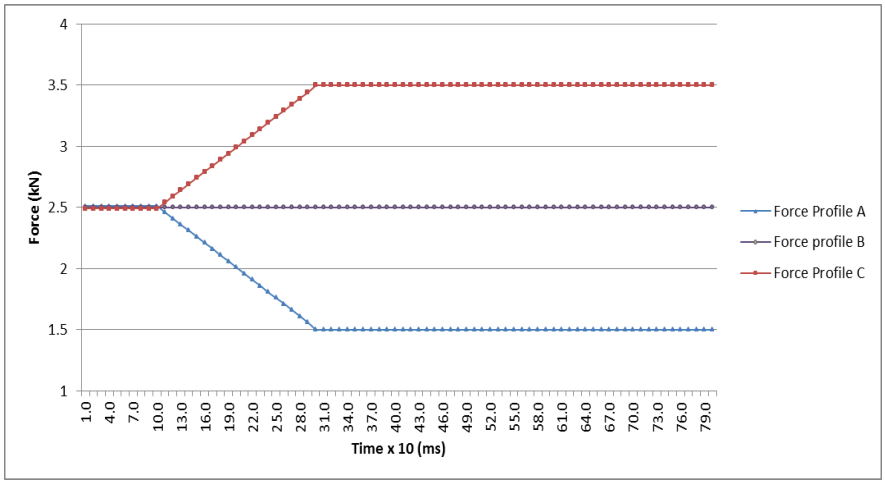


**Figure 3: Force profiles during welding**

## II. RESULTS AND DISCUSSIONS

### *A. Evaluation of Force Control during Welding*

Figure 4 shows the force control during weld cycle for each force profiles within a preset tolerance band. A tolerance band of ± 0.2 kN was given to each force profile to take into account the noise that will be generated during the weld cycle. The source of the noise would be from the machine transformer as well as the servo motor amplifier and will interfere with the piezoelectric signal. A low pass filter has been added to suppress the effect of the noise. Four repetitions were carried out for each force profile to evaluate the repeatability of force control system as well as to evaluate the performance of the control system.

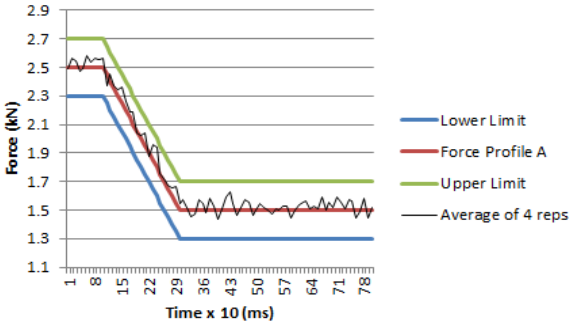


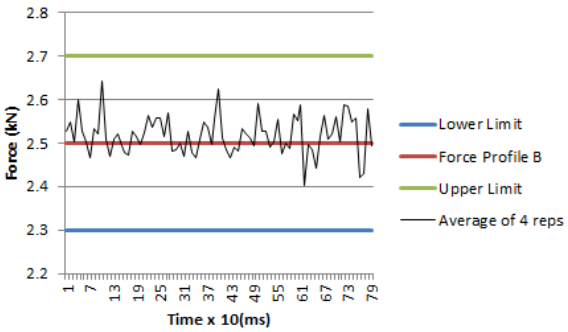

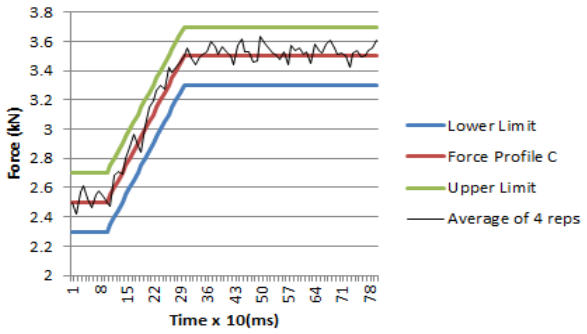


**Figure 4: Electrode force control during welding**

In Figure 4, it is apparent that the developed PID controller was able to control the electrode forces during weld cycle to follow the force profiles within the set tolerance band.

*B. Dynamic Resistance Curves*

In order to analyse the effect of the force profiles on heat generation during welding and weld nugget growth, the dynamic resistance curve for each force profile was generated. The dynamic resistance was calculated from the secondary welding current and secondary voltage across electrodes. The welding current waveform was measured using a toroidal coil that gives a voltage signal proportional to the induced current waveform at the lower arm of the spot welder. Two leads that are connected to both the electrodes will measure the voltage waveform across these electrodes. The dynamic resistance during the process was calculated based on the maximum current value from the current waveform for each half cycle (10 ms) and it's respective voltage value (instantaneous value) from the voltage waveform. Using instantaneous values were found to eliminate the inductive noise resulting in pure resistance values [11].

The force profiles show significant differences between dynamic resistance curves as shown in Figure 5. The starting resistances for the dynamic resistance curves A, B and C are close to each other as their corresponding force profiles have a same starting electrode force of 2.5 kN. However, after 100 ms (vertical line), as electrode forces in the force profiles change except for force profile B, distinct variations were noticed for the three resistance curves.

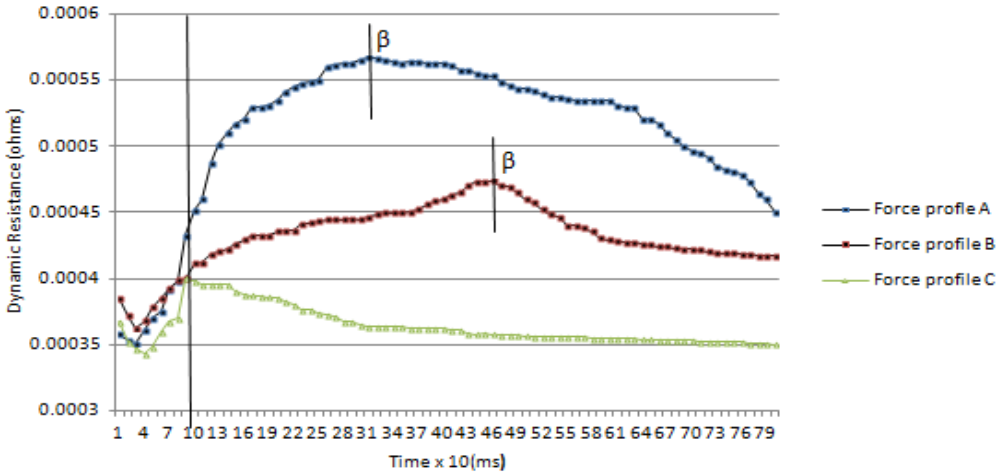


**Figure 5: Dynamic resistance curves for the force profiles**

Dynamic resistance A shows a β-peak occurring earlier compared to dynamic resistance B. As mentioned by Dickinson [9], the β-peak indicates the start of a weld nugget growth. As force decreases to 1.5 kN in force profile A, it led to an increase in resistance which in turn increases heat generation. The melting of metal due to increased Joule heating, initiated a weld nugget growth earlier compared to force profile B, which maintains a constant force. The lower electrode force in force profile A also allowed weld nugget to expand freely and to be fully developed before the end of the weld time. Meanwhile, dynamic resistance C showed the lowest resistance values as the corresponding force profile increased to a higher force of 3.5 kN, which reduced the resistance and in turn the heat required for weld development. As the increase in force suppressed weld nugget growth, no obvious β-peak was noticed for dynamic resistance C. Similar observations were reported in work by Nachimani [12] and Huang [13].

*C. Weld diameter and strength for different force profiles*

Table 1 shows the achieved weld diameter for each force profile. Metallographic samples were produced using standard metallographic procedure. Optical microscopy was used to examine the fusion zones (FZ) in these samples which have coarse macrostructures due to melting and solidification [14]. The weld nugget diameter is represented the width of the FZ. Four metallographic samples were made for each force profile. Figure 6 shows example of a macrostructures which was used to measure weld diameter.

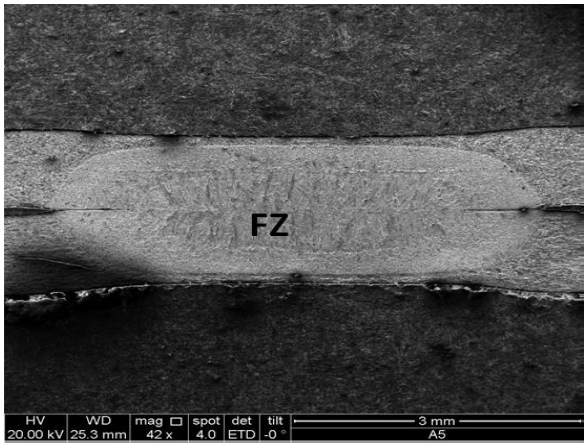


**Figure 6: Examples of macrostructure used to measure weld diameter**

Table 1 also shows the achieved weld strengths for the three different force profiles. The weld strengths were recorded based on tensile tests that were carried out using Lloyd tensile testing machine with a crosshead speed of 10 mm/min. The averages for all results were based on 4 repetitions.

**Table 1: Weld diameters, strengths and failure for different force profiles**

| Force profile | Average weld diameter(mm) | Std.dev | 99% confidence interval | Average weld strength (kN) | Std. dev | 95% confidence interval | Weld failure |
|---|---|---|---|---|---|---|---|
| A | 5.7 | 0.304 | 5.31<μ<6.01 | 10.83 | 0.212 | 10.40<μ<11.28 | Button pullout |
| B | 4.6 | 0.251 | 4.27<μ<4.85 | 9.98 | 0.255 | 9.46<μ<10.21 | Button pullout |
| C | 3.8 | 0.238 | 3.50<μ<4.06 | 6.57 | 0.357 | 5.84<μ<7.31 | Interfacial |

Force profile A (2.5 kN – 1.5 kN) have produced the biggest weld diameter (5.7 mm) and highest weld strength (10.83 kN) compared to the rest of the force profiles. Comparing force profile A and B, which is a constant force profile of 2.5 kN, ramping down the electrode force during the weld cycle for force profile A at 100 ms at the rate of 1 kN/100ms has facilitated the development of spot weld nugget due to a lower electrode force and higher dynamic resistance, as shown by dynamic resistance curve A in Figure 5. Therefore, Profile A achieved a greater weld diameter and higher weld strength compared to Profile B. Work by Iyota [15], which carried out simulations to determine the weld diameters achieved with constant electrode force and electrode force reduced during welding, supports the mentioned observation. However with the use of force profile A, slight expulsion was noticed during the weld cycle mainly due to the reduction in electrode force in the mid of the weld cycle. Fortunately the expulsion did not affect the weld strength. Meanwhile, Profile C (2.5 kN – 3.5 kN) produced the lowest weld strength (6.57 kN) as the electrode force was ramped up to the highest force compared to any of the other force profiles, therefore producing the lowest dynamic resistance as shown by the dynamic resistance curve C (Figure 5) and produced the highest restriction to spot weld initiation and growth.

Two types of weld failure were also observed in this work. Force profiles A and B produced button pullout failures while force profile C produced interfacial failure as shown in Figure 7. With reference to findings by Pouranvari and Ranjbarnoode [16], the weld diameter produced by force profile C was below a critical FZ size.

Therefore the shear stress was greater than the tensile stress, hence created a failure at the interface of the metal sheets. Meanwhile the weld diameters of force profiles A and B were above the critical FZ size, leading to pull-out failures. This work however did not determine the critical FZ size.


**Figure 7: Weld failures produced by the force profiles**

## III. CONCLUSIONS

The reported work has introduced electrode force as a control parameter. The electrode force during welding can be controlled with the use of servomechanism. The evaluation of the electrode force control during weld cycle showed that the control system was able to follow the given force profiles within the pre-set tolerance band. Controlling the electrode force using different force profiles also showed differences in dynamic resistance curves and affected weld nugget growth. Decrease in electrode force during welding was found to increase resistance which in turn increased Joule heating and facilitated weld nugget growth. On the other hand, increase in electrode force during welding, decreased resistance and therefore caused lower Joule heating and impeded weld nugget growth. This work also observed variation in weld failure mode for the different force profiles Reducing the electrode force or maintaining the electrode constant caused welds to fail in the button pull-out mode while

increasing electrode force during welding led to interfacial failure of welds.

## REFERENCES

[1] A Aravinthan and C. Nachimani, "Analysis of spot weld growth on mild and stainless steel", Welding Journal, 90, 2011, pp 143-147.

[2] S.Aslanlar, A.Ogur, U.Ozsarac and E.Ilhan.E, "Effect of welding current on mechanical properties of galvanized chromided steel sheet in electrical resistance spot welding", Materials and Design, 28, 2007, pp 2-7.

[3] M.Pouranvari and S.P.H Marashi, "Factors affecting mechanical properties of resistance spot welding", Materials Science and Technology, 261, 2010, pp 1137-1144.

[4] X.Zhang, G.Chen, Y.Zhang and X.Lai, "Improvement of resistance spot weldability for dual-phase (DP600) steel using servo gun", Journal of Materials Processing Technology, 2009, pp 2671-2675.

[5] P.Briskham, N.Blundell, L.Han and R.Hewitt, "Comparison of self-pierce riveting, resistance spot welding and spot friction joining for aluminum automotive sheet", SAE International, 2006, 2006-01-0774.

[6] P.S.Wei and T.H.Wu, "Electrical contact resistance effect on resistance spot welding", International Journal of Heat and Mass Transfer, 55, 2012, pp 3316-3324.

[7] B.H.Chang and Y.Zhou, "Numerical study on the effect of electrode force in small-scale resistance spot welding", Journal of Materials Processing Technology, 139, 2003, pp 635-641.

[8] W.Tan, Y.Zhou, H.W.Kerr and S.Lawson, "A study of dynamic resistance during small scale resistance spot welding of thin Ni sheets", Journal of Physics D:Applied Physics, 37, 2004, pp 1998 -2008.

[9] D.W.Dickinson, J.E.Franklin and A.Stanya, "Characterization of spot welding behavior by dynamic electrical parameter monitoring". Welding Research Supplement, 1980, pp 170-176.

[10] J.Wen, C.S.Wang, G.C.Xu and X.Q.Zhang, "Real time monitoring weld quality of resistance spot welding for stainless steel", ISIJ International, 49(4), 2009, pp 553-556.

[11] J.D.Cullen and N.Athi, "Multisensor fusion for on-line monitoring of the quality of spot welding in automotive industry", Measurement, 41, 2008, pp 412-423.

[12] C.Nachimani.C, "Analyzing the force and current profiles using pneumatic and servo based electrode actuation system for resistance spot welding", Caspian Journal of Applied Sciences Research, 2(8), 2013, pp 38-45.

[13] Y.D.Huang, A.Pequegnat, J.C.Feng and M.I.Khan, "Resistance microwelding of crossed Pt–10Ir and 316 LVM stainless steel wires", Science and Technology of Welding and Joining, 16(7), 2011, pp 648-656.

[14] .K.Rajkumar, H.Fatin and C.Nachimani, "Investigating the dissimilar weld joints of AISI 302 austenitic stainless steel and low carbon steel", International Journal of Scientific and Research Publications, 2(11), 2012, pp 1-5.

[15] M.Iyota, Y.Mikami, T.Hashimoto, K.Taniguchi and R.Ikeda, "Effect of electrode force condition on nugget diameter and residual stress in resistance spot welded high-strength steel sheets", Journal of Physics: Conference Series 379, 2012, pp 1-9.

[16] M.Pouranvari and E.Ranjbarnoode, "Effect of electrode force on fracture type of DQSK steel resistance spot welds", Acta Metallurgica Slovaca,19(2), 2013, pp 149-153.

## AUTHORS

**First Author** – Aravinthan Arumugam PhD, KDU University College, Malaysia, email: draravinth.a@gmail.com
**Second Author** – Abdul Aziz Baharuddin BEng (Hons) Mechanical Engineering, Nottingham University Malaysia Campus, email: azizbhrd@yahoo.com